Investigation of Manganese Ion Removal from Waters Using Sewage Sludge Ash

İrdemez, Şahset*+; Yeşilyurt, Duygu; Ekmekyapar Torun, Fatma
Atatürk University, Department of Environmental Engineering, 25240, Erzurum, TURKEY

Kul, Sinan
Bayburt University, Department of Emergency Aid and Disaster Management, 69000, Bayburt, TURKEY

Bıngül, Züleyha
Iğdır University, Department of Environmental Engineering, 76000, Iğdır, TURKEY

ABSTRACT: *In this study, the removal of Mn^{2+} ions from waters by the adsorption method using ash obtained from a treatment plant sludge burning unit, which is treatment plant waste and mostly disposed of in a landfill, was investigated. By determining the most suitable conditions for adsorption, adsorption kinetics, isotherms, and thermodynamic values were determined. In the experiments, 63.9% removal efficiency was achieved using 10 g/L adsorbent concentration for 10 mg/L Mn^{+2} under optimum conditions. As a result of the research, it was determined that the adsorption proceeds according to the pseudo-second-degree reaction and abides by the Langmuir isotherm. The thermodynamic constants of $\Delta H°= -4.866$ kJ/mol and $\Delta S°= 21.44$ J/mol were determined. As a result of this, the reaction was exothermic, spontaneous, and random, and adsorption was physical adsorption. As a result of the study, sewage sludge ash can be used in the treatment of water containing low concentrations of Mn^{2+}.*

KEYWORDS: *Adsorption, Manganese removal, Sewage sludge ash, Isotherm, Adsorbent.*

INTRODUCTION

Elements with an atomic weight of 50 g/mol and a density greater than 5 g cm^{-3} are called heavy metals [1-4]. There are nearly 70 heavy metals [5-7]. Even if heavy metals enter the body in trace amounts, they accumulate over time and reach dangerous doses as they are excreted in limited amounts from the body. Mode of ingestion not only affects the type of tissue they accumulate in, but also their toxic effects [7-14].

Manganese is a heavy metal with an atomic number of 25 and an atomic weight of 54.938 [15]. Manganese is a pollutant that is difficult to remove from drinking water due to its natural occurrence and multiple oxidation forms (Mn (II), Mn (III), Mn (IV)). If high Mn concentrations found in water distribution systems are not removed, color change is generally observed after water containing oxidized Mn reaches the consumers' home [16]. Manganese gives a blackish-brownish color to water and creates a metallic taste in water [17]. Manganese is usually

found in surface water in the form of Mn^{2+}. In addition to being toxic to humans, the high amount of Mn^{2+} in water causes problems such as an unpleasant metallic taste in the water, clogging of pipes and causing color changes in clothes [18-21]. Therefore, the removal of Mn ions from water is an important issue [22-26].

Many different methods such as chemical precipitation, adsorption, reverse osmosis, membrane filtration and ion exchange were used in the treatment of - wastewater containing manganese [27-33]. Among these methods, the adsorption method stands out due to its advantages [34]. It is particularly effective in the treatment of waters containing low concentrations of Mn. In addition, studies were carried out to reduce the cost by using many different adsorbent types [35]. Unlike these, activated carbon is the most commonly used adsorbent, although it is expensive [36].

In recent years, the issues about disposal and treatment of sewage sludge have received rising concern from the public [37]. It is difficult to dispose of large quantities of sewage sludge produced from sewage treatment plants. If sewage sludge is not disposed of appropriately, it causes environmental impacts and health problems [38, 39]. SSA from incineration facilities is primarily an inorganic and stable material [40, 41]. SSA predominantly contains silicon oxide and aluminum oxide. The weight ratio of these two compounds in SSA is primarily between 31.5 and 70.8% [42, 43].

Due to the relatively low molecular weight of manganese ions, they are more difficult to remove from water compared to other heavy metals. Due to this feature, adsorption studies about Mn^{2+} removal are very limited in the literature. In this study, the removal of Mn^{2+} ions from water was investigated by using SSA, which is a treatment plant waste. The SSA used was obtained from the domestic wastewater treatment plant belonging to Gaziantep province. The adsorbent is very advantageous because it is a treatment plant waste. In this study where the adsorption method was used; the effects of parameters such as time, pH, temperature, concentration, stirring speed and adsorbent amount were investigated. By examining the adsorption kinetics and fit of the results to the isotherm equations, the isotherm constants and reaction degree were determined. In addition, thermodynamic studies were carried out and the values were determined for thermodynamic parameters.

EXPERIMENTAL SECTION
Materials
SSA used in the experiments was obtained from the incineration unit of the domestic wastewater treatment plant in Gaziantep. SSA was supplied in powder form and used. Later, SSA to be used as adsorbent was mixed with HCl acid solution in the reactor so that the pH value remained constant at 4.5 and after the pH reached 4.5, it was washed in pure water. The washed SSA was then dried in the oven during 24 h at 100 °C.

Methods
Adsorption experiments were carried out in an incubator hood TH (Edmund Buhler GmbH) shaker by placing synthetically prepared 100 mL of wastewater containing manganese in 250 mL flasks. Analyses of samples taken at certain time intervals were made using manganese test kits. Experiments were made with 3 repetitions and their arithmetic mean was calculated.

In adsorption kinetics studies, pseudo first order and pseudo second order reaction kinetic equations developed for heterogeneous reactions were used to determine the reaction rate [44-47].

Pseudo first order reaction kinetics equation;

$$\ln(q_e - q_t) = \ln q_e - k_1 * t \tag{1}$$

Pseudo second order reaction kinetics equations;

$$\frac{t}{q_t} = \frac{1}{q_e^2 * k_2} + \frac{t}{q_e} \tag{2}$$

$$q_e = \frac{C_o - C_e}{m} \tag{3}$$

$$q_t = \frac{C_o - C}{m} \tag{4}$$

The Arrhenius equation given in Eq. 5 was used to calculate the activation energy.

$$\ln k_2 = -\frac{E_a}{R} * \frac{1}{T} + \ln Z_e \tag{5}$$

To find the Gibbs free energy from the data obtained as a result of experiments at different temperatures, Eq. 6 was used.

$$K_c = \frac{C_a}{C_e} \tag{6}$$

$$\Delta G^o = -R * T * \ln(K_c) \tag{7}$$

Enthalpy and entropy values can be calculated from Eq. 7.

$$\ln K_c = \frac{\Delta S^o}{R} + \frac{\Delta H^o}{R*T} \qquad (8)$$

Freundlich, Langmuir, BET and Temkin isotherm equations were used to determine the equilibrium state between the adsorbent and the adsorbate at constant temperature. Freundlich, Langmuir, BET and Temkin isotherm equations are given in Eqs. 9-12, respectively [48-55].

$$\ln q_e = \ln K_F + \frac{1}{n} . \ln C_e \qquad (9)$$

$$\frac{1}{q_e} = \frac{1}{a.K_L} . \frac{1}{C_e} + \frac{1}{a} \; ; \; R_L = \frac{1}{1 + K_L * C_0} \qquad (10)$$

$$\frac{C_e}{(C_s - C_e).q_e} = \frac{1}{K_B q_s} + \frac{K_B - 1}{K_B.q_s} . \frac{C_e}{C_s} \qquad (11)$$

$$q_e = \frac{R.T}{b_T} . \ln K_T + \frac{R.T}{b_T} . \ln C_e \; ; \; B = \frac{R.T}{b_T} \qquad (12)$$

Characterization studies

SEM, FT-IR and XRD analyses were performed to characterize SSA used as adsorbent. Morphological features of the adsorbents were obtained with a Zeiss Sigma 300 Scanning Electron Microscope (SEM). All samples were glued to a sample stub and covered with 10 nm gold-palladium layer for the SEM images. X-ray diffraction data were obtained using Bruker D8 Discover XRD device to determine the structural features of adsorbents.

RESULTS AND DISCUSSION

Parameters affecting of adsorption of Mn²⁺ ions using SSA

In the study about removing Mn^{2+} ions from water by the adsorption method using SSA, the effects of initial pH of water, adsorbent concentration, stirring speed and temperature were investigated on adsorption. The results of the experiments are given in Fig. 1. While examining the parameters affecting adsorption, 10 mg/L Mn^{2+}, 20 °C temperature, 200 rpm stirring speed, pH=3 and 10 g/L adsorbent concentration were used, apart from the variation in examined parameters.

It is seen in Fig. 1 that adsorption takes place rapidly after the first contact of the adsorbent and the solution containing Mn^{2+}. The change in Mn removal efficiency with time under optimum conditions is given in Fig. 2. The Mn^{2+} removal efficiencies under optimum conditions reached 48.8% at 10 min, 61.6% at 30 min, 62% at 60 min and 63.9% at the end of 120 min. After 60 min, there was not much increase in removal efficiencies.

In the Mn^{2+} removal studies using SSA as adsorbent, the experiments to examine the effect of pH value on adsorption were carried out at 10 g/L adsorbent concentration, 10 mg/L Mn^{2+} concentration, 20 °C and 200 rpm stirring speed. The results are given in Fig. 1a. The most soluble form of manganese is Mn^{2+} and this form is stable under acidic conditions and readily oxidized under basic conditions. In neutral and acidic aqueous solutions, the Mn^{2+} cation turns into $Mn(H_2O)_6^{-2}$. Oxidation increases and solubility decreases as the hydroxide ion in the environment increases [56]. Since the pH where $Mn(OH)_2$ begins to occur is around 6, it is not possible to determine whether the increase in efficiency above this pH is due to adsorption or chemical precipitation, so there was no study above this pH because $Mn(OH)_2$ is a weakly amphoteric base with low water solubility. For these reasons, Mn removal by the adsorption method is higher in weak acidic conditions. When pH <3, removal efficiency decreases due to high H^+ ions in the solution. As a result of the experiments, while the highest removal efficiency was obtained at pH 3, the next highest efficiency was obtained at pH 4. It was decided that the optimum working pH is between 3-4.

In the Mn^{2+} removal studies using SSA as adsorbent, the experiments to examine the effect of adsorbent concentration on adsorption were carried out at pH 3, 20 °C and 200 rpm. The results of studies with different adsorbent concentrations are shown in Fig. 1b. As can be seen in Fig. 1b, 16.78% removal efficiency was achieved when 1 g/L adsorbent concentration is used to treat water containing 10 mg/L Mn^{2+} by using SSA. Removal efficiency reached 63.9% when 10 g/L adsorbent concentration was used.

High adsorbent dosage should be used in order to achieve sufficient efficiency for Mn^{2+} removal. So, the q_e values obtained for the removal of Mn^{2+} using SSA are very low. In fact, in studies apart from Mn^{2+}, attempts were made to use many heavy metals (Zn, Ni, etc.) for removal, but removal could not be obtained. Due to these results, it is possible to use SSA in the removal of water with low Mn^{2+} content.
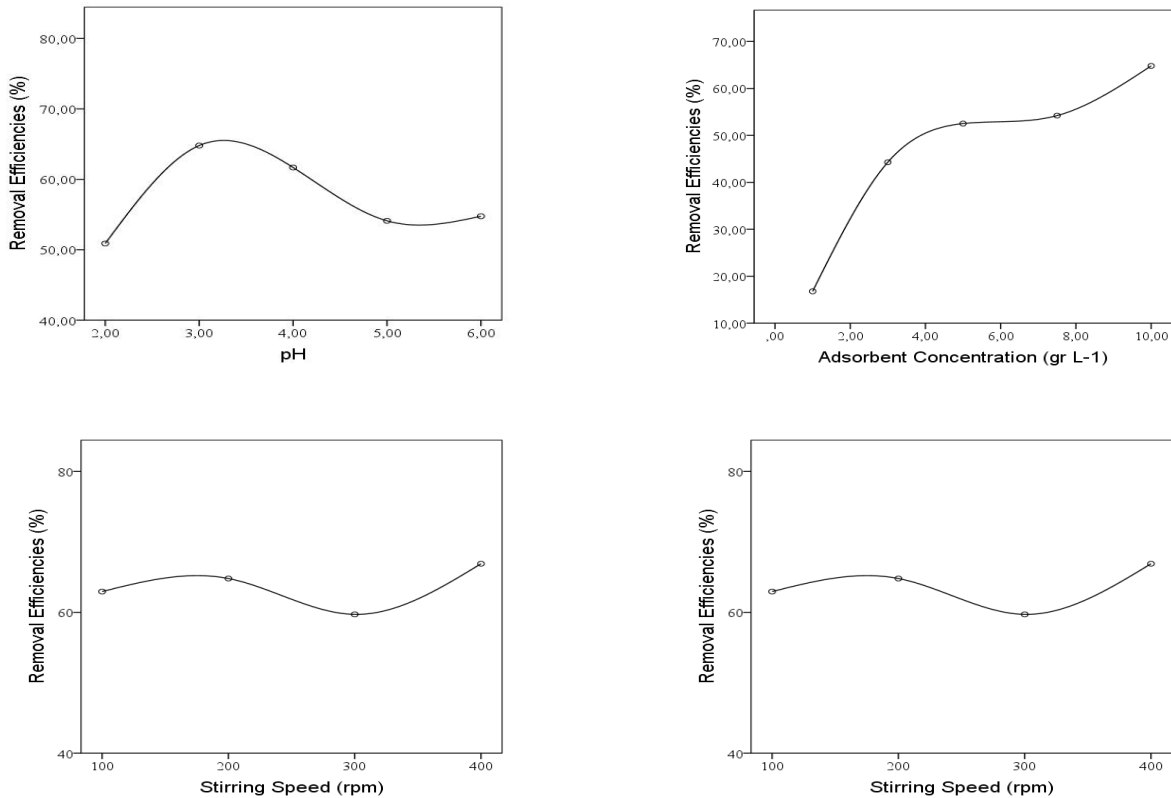
Fig. 1: Parameters affecting the removal of Mn²⁺ions using SSA a) effect of pH b) effect of adsorbent concentration c) effect of stirring speed d) effect of temperature
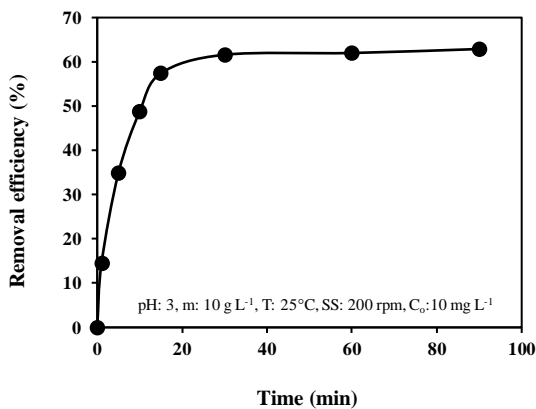

Fig. 2: Change in Mn²⁺ removal efficiency with time under optimum conditions.

The experiments to investigate the effect of stirring speed on adsorption were carried out at 10 mg/L Mn^{2+}, 10 g/L adsorbent concentration, 20 °C and pH 3. The results obtained in the experiments with different stirring speeds are shown in Fig. 1c. When Fig. 1c is examined, the time to equilibrium for adsorption is 60 min at 100 rpm,

45 min at 200 rpm, 30 min at 300 rpm and 15 min at 400 rpm. When this period is prolonged, desorption occurs at 300 rpm and 400 rpm. While the removal efficiency obtained at 200 rpm is 63.9%, the removal efficiency increases to 66.9% when the stirring speed is doubled. However, the desorption rate was much higher at 400 rpm compared to 200 rpm, and stability could not be achieved for the effluent concentration. Considering both this reason and the cost of mixing, it was concluded that 200 rpm is more suitable for operation.

The experiments to investigate the effect of temperature on adsorption were carried out at an initial concentration of 10 mg/L Mn^{2+}, an adsorbent concentration of 10 g/L, a stirring speed of 200 rpm and pH 3. The change in the removal efficiency with time was obtained in studies conducted at different temperatures is shown in Fig. 1d. When Fig. 1d is examined, the temperature does not have much effect on adsorption after 120 min of contact time.

While the efficiency of removal at 20 °C was 63.9%, it was determined as 63.87% at 30 °C, 63.77% at 40 °C
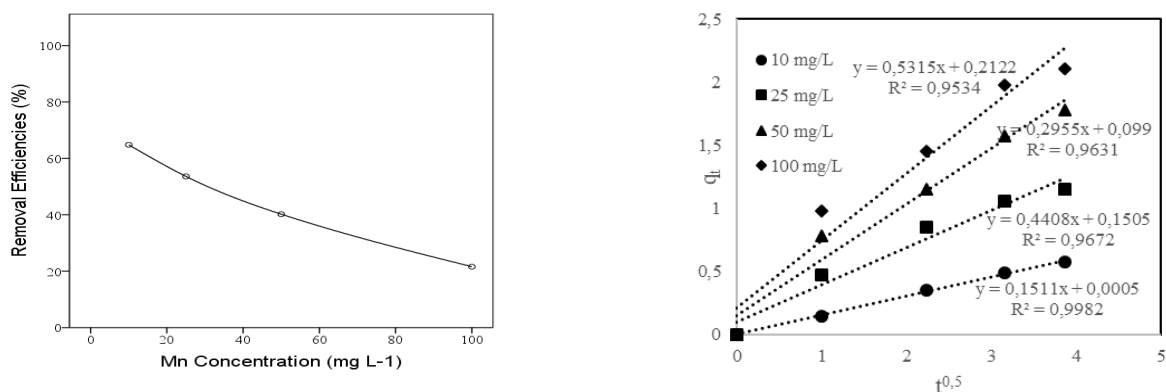
Fig. 3: a) Results for adsorption experiments performed with different Mn^{2+} concentrations and
b) the pore diffusion plot drawn for the first 15 min.

and 63.02% at 50 °C. As the temperature increases, the reaction rate increases. Reaction rate constant were calculated as 0.4736 g/mg.min for 20 °C, 0.4817 g/mg.min for 30 °C, 0.681 g/mg.min for 40 °C and 0.872 g/mg.min for 50 °C.

The results of the adsorption experiments performed with different Mn^{2+} concentrations and the pore diffusion plot drawn for the first 15 min are given in Fig. 3. The experiments were carried out at 20 °C with an adsorbent concentration of 10 g/L at 200 rpm.

When Fig. 3a is examined, the removal of Mn^{2+} ions with SSA is more efficient for low manganese concentrations. Much higher concentrations of adsorbents should be used for high manganese concentrations. The results obtained from the experiments show that adsorption is controlled by pore diffusion for the first 10-15 min and later, adsorption is controlled by liquid film diffusion as the concentration of Mn^{2+} in the solution decreases, as seen in Fig. 3b.

Since SSA is a multicomponent substance, the zeta potential also differs in different zones. In other words, the surface electrical charge of SSA at different pHs can have different charges in different regions. Negative regions on SSA can attract Mn^{2+} ions. In this case, electrostatic attraction ensures adsorption [43]. Adsorbent characterization performed before and after adsorption showed that the concentration of some ions decreased. In the analyses performed before and after adsorption, the amount of oxygen decreased from 43.84% to 40.87%, the amount of Ca from 25.36% to 20.71% and the S percentage from 18.61% to 13.61%. This case indicates ion exchange adsorption.

Adsorption kinetics for removal of Mn^{2+} ions using SSA

Pseudo first order and pseudo second order kinetic graphs were drawn with the data obtained from studies to examine the effect of the amount of adsorbent. The graphs obtained are given in Fig. 4. The reaction rate constants obtained from these results are shown in Table 1.When Fig. 4 and Table 1 are examined, the adsorption mechanism of Mn^{2+} removal occurs according to the pseudo second order reaction kinetics. This is because both the results obtained from the experimental data are in accordance with the pseudo second order kinetic equation and the obtained q_e values are closer to the real q_e values.

Adsorption isotherm for removal of Mn^{2+} ions using SSA

Calculations of isotherms were carried out with the data obtained from the studies to examine the effect of the amount of adsorbent. Freundlich, Langmuir BET and Temkin isotherms drawn according to the results are shown in Fig. 5.

The isotherm coefficients calculated with the results obtained from Fig. 5 are given in Table 2. When the R^2 values given in Table 2 are examined, the Langmuir isotherm model is better than the other isotherm models. The value of a in the Langmuir isotherm indicates the maximum adsorption capacity of the adsorbent and K_L indicates the Langmuir constant.

When the R^2 values given in Table 2 are examined, the Langmuir isotherm model is better than the other isotherm models. The value of a in the Langmuir isotherm indicates the maximum adsorption capacity of the adsorbent and K_L indicates the Langmuir constant. To describe other

Table 1: Reaction rate constants for different adsorbent concentrations for removal of Mn^{2+} ions using SSA.

m (g/L)	$q_{e,real}$ (mg/g)	Pseudo first order, k_1 (min⁻¹)	$q_{e, exp}$ (mg/g)	Pseudo second order, k_2 (g/mg.min)	$q_{e, exp}$ (mg/g)
1	1.775	0.0352	0.955	0.089	1.850
3	1.617	0.0471	0.793	0.110	1.247
5	1.17	0.0653	0.602	0.395	1.184
7.5	0.833	0.1155	0.612	0.453	0.845
10	0.648	0.1008	0.508	0.501	0.658

Table 2: Isotherm constants for Mn^{2+} adsorption by SSA at 30 °C.

Freundlich isotherm constants			Langmuir isotherm constants		
K_F	n	R^2	K_L	a	R^2
0.4971	0.8695	0.9518	$7.01*10^{-3}$	37.87	0.9609
BET isotherm constants			Temkin isotherm constants		
K_B	q_s	R^2	K_T	b_T	R^2
-4.28	2.94	0.9147	0.844	1141.02	0.9025
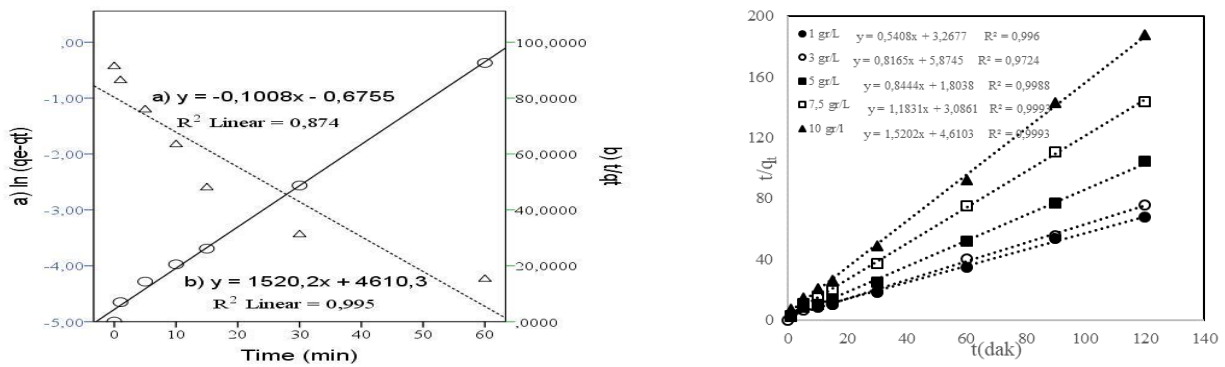
Fig. 4: a) Pseudo first and pseudo second order rate graph b) Pseudo second order rate graph for different adsorbent concentrations using SSA.
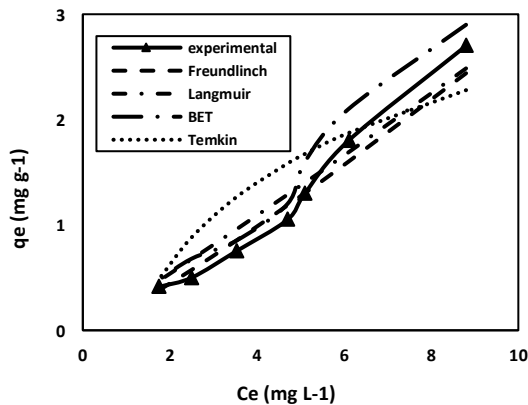
Fig. 5: Adsorption isotherms for Mn^{2+} removal using SSA.
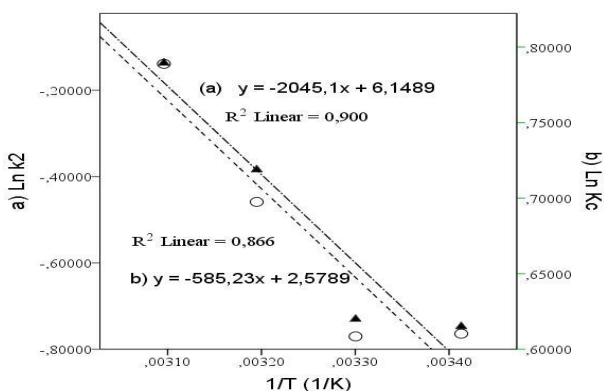
important properties of the Langmuir isotherm, apart from these values, the R_L value given in Eq. 9 was used. If $R_L>1$, adsorption is not suitable; if $R_L=1$, it is linear; if $0<R_L<1$, adsorption is suitable; or if $R_L=0$, the process is irreversible [57]. As a result of the calculations with the help of Eq. 9, the R_L value was found to be 0.9345 and adsorption is suitable according to the Langmuir isotherm.

Calculation of thermodynamic constants for the adsorption of Mn^{2+} ions

The activation energy of adsorption and other thermodynamic constants were calculated using the results obtained from the experiments to determine the effect

Table 3: Activation energy and thermodynamic constants for Mn²⁺ removal using SSA.

T (K)	$\Delta G°$ (kJ/mol)	$\Delta S°$ (J/mol.K)	$\Delta H°$ (kJ/mol)	k_2 (g/mg.min)	E_a (kJ/mol)
293	-1.487			0.4736	
303	-1.482	21.44	-4.866	0.4817	17,003
313	-1.699			0.6810	
323	-1.922			0.872	

Fig. 6: Graphs drawn to find activation energy a) and thermodynamic constants b) for Mn²⁺ removal using SSA.

of temperature on the removal of Mn²⁺ ions with SSA. Linear graphs in Fig. 6, drawn using Eq. 8, were used to determine thermodynamic constants and activation energy values. The values calculated using Eq. 7 and Fig. 6 are given in Table 3.

The negative $\Delta H°$ value indicates that the reaction is exothermic, and the negative $\Delta G°$ value indicates that the adsorption process is spontaneous. The negative increase in $\Delta G°$ with increasing temperature indicates that the adsorption process occurs more spontaneously as the temperature increases. The positive $\Delta S°$ value indicates that the adsorption process is random [58]. If the activation energy is between 5 kJ/mol and 40 kJ/mol , adsorption is defined as physical adsorption [59, 60]. When the activation energy is examined, it can be said that adsorption is physical adsorption and occurs rapidly.

In a study by *Nie et al.* [61] about lead removal using SSA, $\Delta S°= 137.81$ J/mol and $\Delta H°=38.91$ kJ/mol were obtained. In Ni and Cd removal studies conducted by *Elouear et al.* [62] using SSA, entropy values were 101.21 J/mol for Ni²⁺ and 132.6 J/mol for Cd²⁺. Enthalpy values were determined as 10.17 kJ/mol for Ni and 18.9 kJ/mol for Cd. Since the molecular weight of Mn²⁺

ions is lower than that of Cd²⁺, Pb²⁺ and Ni²⁺ ions, they have high affinity for water and are difficult to remove by adsorption. This is the main reason for the low q_e values obtained.

Statistical tests

The effect level of the parameters were studied in the IBM SPSS statistic 20 program and the values given in Table 4 were obtained.

Since the eta square values given in the table are greater than 0.138, all the studied parameters are effective on the treatment efficiency [63-65]. However, considering that the effect level increases as the eta square value increases, it can be said that the most effective parameters are adsorbent concentration, adsorbate concentration and pH.

Adsorbent characterization

The adsorbents before and after the experiments were examined with the XRD device and the diagram given in Fig. 7a was obtained. X-Ray diffraction analysis for samples of SSA by Bruker D8 Discover XRD device was examined with 2Ө angle in the range 10- 90 using 40 kV and 40 mA operating values.

When Fig. 7a is examined, the obtained sharp peaks have a high degree of crystalline structure for SSA. In general, peaks obtained in 4 different cases are similar to each other. This demonstrates that the chemical reactions between the adsorbent and Mn²⁺ ions are limited and the adsorption of Mn²⁺ions had a negligible effect on the crystal phases of the adsorbent [66].

In the literature, for characterization studies of SSA, the basic structure of this substance consisted of SiO_2, Al_2O_3, Fe_2O_3, CaO, P_2O_5, SO_3, Na_2O, K_2O, TiO_2, MgO and MnO. The remaining part is composed of As, Ba, Cd, Co, Cr, Cu, Hg, Ni, Pb, Sn, Sr, V, and Zn at ppm level [67-68]. However, the content of SSA varies considerably according to the treatment processes used, the type of sludge and the characteristics of the incinerator. While

Table 4: Univariate tests performed using IBM SPSS statistics 20 program.

Source	Type III Sum of Squares	df	Mean Square	F	Sig.	Partial Eta Squared
Corrected Model	20078.015[a]	17	1181.060	703.882	.000	.994
Intercept	44235.983	1	44235.983	26363.550	.000	.997
pH	795.440	4	198.860	118.516	.000	.860
m	8008.716	4	2002.179	1193.249	.000	.984
Stirring speed	124.146	3	41.382	24.663	.000	.490
Temperature	130.033	3	43.344	25.832	.000	.502
Adsorbate concentration	6463.660	3	2154.553	1284.060	.000	.980
Error	129.200	77	1.678			
Total	305057.783	95				
Corrected Total	20207.215	94				
a. R Squared = ,994 (Adjusted R Squared = ,992)						

SSA structure used in this study contained high amounts of Si, Ca, S and O, other substances were present in trace amounts. The amount of these substances decreased after adsorption.

FT-IR images of SSA before experiments and after Mn^{2+} removal are given in Fig. 7b. When before and after adsorption are compared, peaks at 1008, 1112 and 3605 wavelengths disappeared after adsorption. The biggest differences between the peaks before and after adsorption are seen as an increase of 3.6% at 598 cm^{-1} and the shift of the peak at 1089 cm^{-1} to 1104 at the end of adsorption and 1.84% increase in % T. The adsorption characteristics of sulfate ions in combination with stretching vibrations of Si-O bonds appear in the region of 1281–841 cm^{-1}. The bands from 1708 to 1576 cm^{-1} correspond to the O-H bending vibrations of H_2O molecules. Stretching vibrations of Fe-O bonds appear in the region of 648–515 cm^{-1}. The overlapping bands in the region from 3660 to 3120 cm^{-1} correspond to the stretching vibrations of Al-OH groups and O-H bonds within hydrogen bonded groups [69].

SEM images magnified by 10000 times are also given in Fig. 7c and 7d. The SSA sample consisted of aggregated small particles with very irregular shapes from the analysis of the scanning electron micrograph. These shapes are quite common in incinerated ash.

The SSA had porous and irregular-shaped particles. The micrographs displayed in Fig. 7d show topographic changes following adsorption. The surface forms much denser and much more uniformly stacked crystal phases.

CONCLUSIONS

In this study, the parameters effective on adsorption and removal of Mn^{2+} ions from synthetically prepared wastewater by using ash from the incineration unit of the domestic wastewater treatment plant of Gaziantep were investigated.

In the studies, the effect of pH was examined at low pHs. The effect of pH in adsorption studies was investigated at low pHs and pH 3 was obtained as the most suitable solution pH. When the pH is raised above 6.5, Mn^{+2} ions combine with hydroxide (OH^-) ions in water and precipitate, and the chemical precipitation mechanism becomes the effective process instead of adsorption.

In the experiments investigating the effect of adsorbent concentration, sufficient efficiency could not be obtained at low adsorbent concentrations. For 10 mg/L Mn^{2+} concentration, 63.9% removal efficiency was obtained at 10 g/L adsorbent concentration. Since Mn^{2+} ions are found in low concentrations especially in drinking water and these low concentrations are difficult to reduce with other processes, it is thought that treatment with sludge ash will be a good option for manganese removal from drinking water.

In the experiments where the effect of stirring speed was investigated, studies were carried out at 100, 200, 300 and 400 rpm. Although relatively higher removal efficiency was obtained at 400 rpm, it was concluded that 200 rpm provided more reproducible results since stability in the output concentration could not be achieved due to desorption.
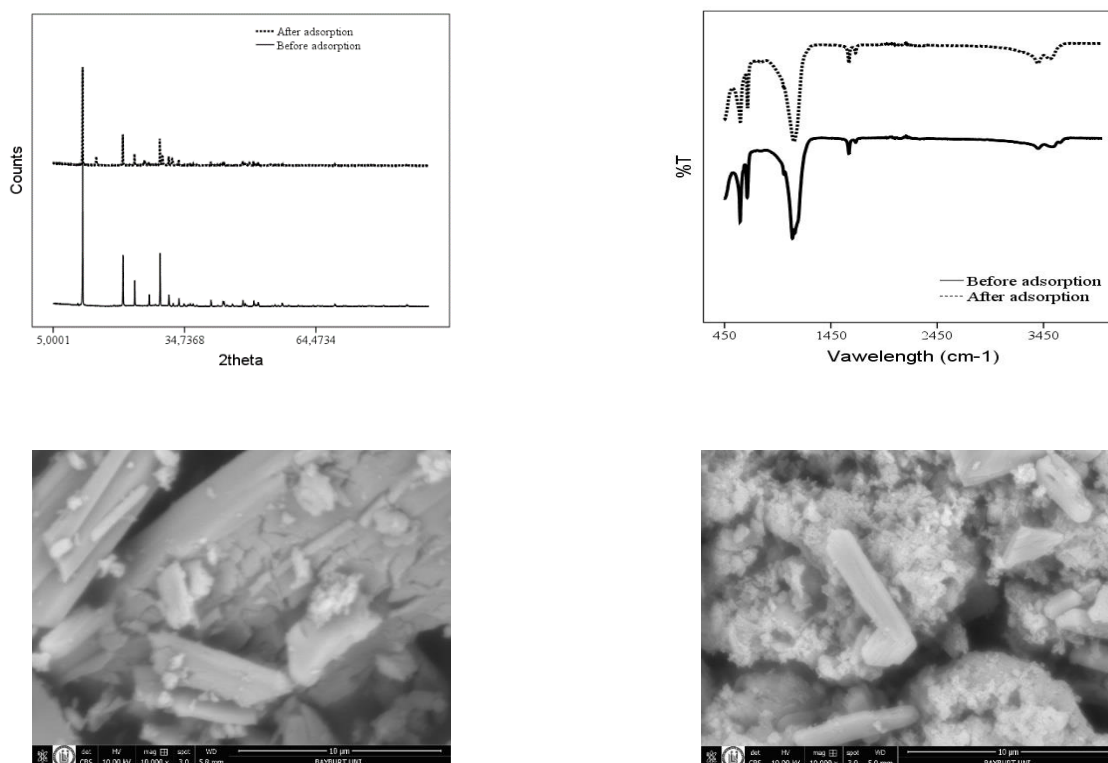
Fig. 7: a) XRD diagram of SSA before and after adsorption b) FTIR images of SSA before and after manganese removal c) SEM images of SSA before the experiment d) SEM images of SSA after Mn^{2+} removal.

Then, kinetic studies were conducted and the reaction degree was determined by applying the obtained data to pseudo-first-order and pseudo-second-order kinetics. As a result of these investigations, the reaction proceeded in accordance with the pseudo second degree kinetics. According to the pseudo second degree kinetics, the reaction rate constant was determined as 0.4736 g/mg.min at 20 ºC.

As the temperature increases in Mn^{2+} adsorption, there was not much change in efficiency. As a result of the calculations, the reaction enthalpy and reaction entropy of Mn^{2+} adsorption were determined as $\Delta H° = -4.866$ kJ/mol and $\Delta S° = 21.44$ joule/mol.K. If $\Delta H°$ is negative, the reaction is exothermic, and if $\Delta G°$ is negative, it indicates that adsorption occurs spontaneously. The positive $\Delta S°$ indicates that randomness is high. The activation energy of the reaction was found to be 7.003 kJ/mol. This shows that Mn^{2+} adsorption is physical adsorption.

As a result of the tests, the effect degree of the parameters affecting adsorption was determined as the amount of adsorbent, pH, temperature and stirring speed, respectively. The data obtained as a result of the studies were applied to Freundlich, Langmuir, BET and Temkin isotherms and kinetic constants were determined for these isotherms. The adsorption for both metal ions fits better to the Langmuir isotherm and the adsorption proceeds in a single layer with the adsorption rate directly proportional to the active sites on the surface. Before and after adsorption XRD, SEM and FT-IR imaging were performed to determine the characterization of SSA. As a result of these, SSA has a porous, irregular and highly crystal structure. There was no change in the crystal structure of the adsorbent after manganese adsorption. SEM images show that Mn ions are retained on the surface.

At the end of this study, it is thought that SSA, which waste from a treatment plant combustion unit, it can be chosen for the treatment of water containing low concentrations of Mn^{2+}. In this case, waste will be used and the Mn removal cost for the treatment plant will decrease.

Numencluture

$\Delta G°$	Gibbs free energy, kJ/mol

ΔH°	Enthalpy, J/mol.K
ΔS°	Entropy, J/mol.K
A	The maximum amount of the adsorbate adsorbed per unit weight of adsorbent, mg/g
b_T	The Temkin constant related to the heat of adsorption, J/mol
C	Heavy metal concentration of the wastewater at time t, mg/L
C_a	Amount of substance retained per unit amount of adsorbent, mg/g
C_e	Adsorbate concentration in solution at equilibrium, mg/g
C_o	Initial heavy metal concentration of wastewater, mg/L
C_s	Saturation concentration of the solute on the adsorbent, mg/L
E_a	Activation energy, kJ/mol
K_B	BET constant expressing the energy of interaction with the surface, L/mg
K_c	The adsorption equilibrium constant
K_F	The Freundlich adsorption constant (adsorption capacity), mg/g
K_L	Constant related to the affinity of adsorbent attachment areas, L/mg
K_T	The Temkin isotherm equilibrium binding constant, L/g
N	The Freundlich adsorption constant adsorption intensity, L/mg
q_e	The amount of adsorbate adsorbed per unit amount of adsorbent at equilibrium, mg/g
q_s	The amount of adsorbate required to form a single layer on the adsorbent surface, mg/g
q_t	Amount of adsorbate adsorbed per unit amount of adsorbent at time t, mg/g
R	The gas constant, 8.3145 J/mol.K
SSA	Sewage sludge ash
T	Temperature, K

REFERENCES

[1] Ali H., Khan E., What are Heavy Metals? Long-Standing Controversy over the Scientific Use of The Term 'Heavy Metals'-Proposal of a Comprehensive Definition, *Toxicological & Environmental Chemistry,* **100(1)**: 6-19 (2018). https://doi.org/10.1080/02772248.2017.1413652.

[2] Jarup L., Hazards of Heavy Metal Contamination, *British Medical Bulletin,* **68(1)**:167-182 (2003). https://doi.org/10.1093/bmb/ldg032.

[3] Barakat M.A., New Trends in Removing Heavy Metals from Industrial Wastewater, *Arabian Journal of Chemistry,* **4(4)**: 361-377 (2011). https://doi.org/10.1016/j.arabjc.2010.07.019.

[4] Jaishankar M., Tseten T., Anbalagan N., Mathew B.B., Beeregowda K.N., Toxicity, Mechanism and Health Effects of Some Heavy Metals, *Interdisciplinary Toxicology*, **7(2)**: 60-72 (2014). https://doi.org/10.2478/intox-2014-0009.

[5] Rahman Z., Singh V.P., The Relative Impact of Toxic Heavy Metals (THMs) (Arsenic (As), Cadmium (Cd), Chromium (Cr)(VI), Mercury (Hg), and Lead (Pb)) on the Total Sewage Environment: an Overview, *Environmental Monitoring and Asses*sment, **191**: 419 (2019). https://doi.org/10.1007/s10661-019-7528-7.

[6] Aslam B., Javed I., Khan H.F., Rahman Z., Uptake of Heavy Metal Residues from Sewage Sludge in the Goat and Cattle During Summer Season, *Pak. Vet. Journal,* **31**: 75-77 (2011).

[7] Duffus J.H., Heavy Metals: A Meaningless Term (IUPAC Technical Report), *Pure. Appl. Chem.*, **74**: 793-807 (2002). https://doi.org/10.1351/pac200274050793.

[8] Yang Y., Ali H., Khan E., Ilahi I., Environmental Chemistry and Ecotoxicology of Hazardous Heavy Metals: Environmental Persistence, Toxicity, and Bioaccumulation, *Journal of Chemistry,* **2019**: 6730305 (2019). https://doi.org/10.1155/2019/6730305.

[9] Men C., Liu R., Xu L., Wang Q., Guo L., Miao Y., Shen Z., Source-Specific Ecological Risk Analysis and Critical Source Identification of Heavy Metals in Road Dust in Beijing, China, *Journal of Hazardous Materials,* **388**: 121763 (2020). https://doi.org/10.1016/j.jhazmat.2019.121763.

[10] Rahman M.S., Khan M.D.H., Jolly Y.N., Kabir J., Akter S., Salam A., Assessing Risk to Human Health for Heavy Metal Contamination Through Street Dust in the Southeast Asian Megacity: Dhaka, Bangladesh, *Science of the Total Environment,* **660**: 1610-1622 (2019). https://doi.org/10.1016/j.scitotenv.2018.12.425.

[11] Lakherwal D., Adsorption of Heavy Metals: A Review, *International Journal of Environmental Research and Development,* **4(1)**: 2249–3131 (2014).

[12] Liu J., Cao L., Dou S., Bioaccumulation of Heavy Metals and Health Risk Assessment in Three Benthic Bivalves Along the Coast of Laizhou Bay, China, *Marine Pollution Bulletin,* **117**: 1–2 (2017). *doi:*10.1016/j.marpolbul.2017.01.062.

[13] Farooq M., Anwar F., Rashid U., Appraisal of Heavy Metal Contents in Different Vegetables Grown in the Vicinity of an Industrial Area, *Pak. J. Bot.,* **40**: 2099-106 (2008).

[14] Wang J., Chen C., Biosorption of Heavy Metals by Saccharomyces Cerevisiae, *Biotechnol. Adv.,* **24**: 427-51 (2006). *doi:*10.1016/j.biotechadv.2006.03.001.

[15] Kul Z.E., Nuhoglu Y., Kul S., Nuhoglu Ç., Torun F.E., Mechanism of Heavy Metal Uptake by Electron Paramagnetic Resonance and FT-IR: Enhanced Manganese(II) Removal onto Waste Acorn of Quercus Ithaburensis, *Separation Science and Technology,* **51(1)**: 115-125 (2016) https://doi.org/10.1080/01496395.2015.1081943.

[16] Chen P., Culbreth M., Aschner M., Exposure, Epidemiology, and Mechanism of the Environmental Toxicant Manganese, *Environ. Sci. Pollution Research,* **23**: 13802–13810 (2016). *doi:*10.1007/s11356-016-6687-0.

[17] Sain A.E., Griffin A., Dietrich A.M., Assessing taste and Visual Perception of Mn(II) and Mn(IV), *JAWWA,* **106(1)**: 32-40 (2014). https://doi.org/10.5942/jawwa.2014.106.0003.

[18] Neculita C.M., Rosa E., A Review of the Implications and Challenges of Manganese Removal from Mine Drainage, *Chemosphere,* **214**: 491-510 (2019). https://doi.org/10.1016/j.chemosphere.2018.09.106.

[19] Cai Y., Li D., Liang Y., Luo Y., Zeng H., Zhang J., Effective Start-Up Biofiltration Method for Fe, Mn, and Ammonia Removal and Bacterial Community Analysis, *Bioresource Technology,* **176**: 149-155 (2015). https://doi.org/10.1016/j.biortech.2014.11.025.

[20] Hoyland V., Knocke W.R., Falkinham J.O., Pruden A., Singh G., Effect of pH on Biological Removal of Manganese in Surface Water Treatment Plants, *Water Research,* **66:**31-39 (2014). https://doi.org/10.1016/j.watres.2014.08.006.

[21] Li C., Wang S., Du X., Cheng X., Fu M., Hou N., Li D., Immobilization of Iron- and Manganese-Oxidizing Bacteria with a Biofilm-Forming Bacterium for the Effective Removal of Iron and Manganese from Groundwater, *Bioresour. Technol.,* **220**: 76–84 (2016). https://doi.org/10.1016/j.biortech.2016.08.020.

[22] Alvarez-Bastida C., Martínez-Miranda V., Solache-Ríos M., Linares-Hernández I., Teutli-Sequeira A., Vázquez-Mejía G., Drinking Water Characterization and Removal of Manganese. Removal of manganese from Water, *Journal of Environmental Chemical Engineering,* **6(2)**: 2119-2125 (2018). https://doi.org/10.1016/j.jece.2018.03.019.

[23] Hsieh S-H., Horng J-J., Adsorption behavior of Heavy Metal Ions by Carbon Nanotubes Grown on Microsized Al_2O_3 Particles, *J. Univ. Sci. Technol. Beijing, Mineral, Metallurgy, Material,* **14(1)**: 77-84 (2007). https://doi.org/10.1016/S1005-8850(07)60016-4.

[24] Stafiej A., Pyrzynska K., Adsorption of Heavy Metal Ions with Carbon Nanotubes, *Microchemical Journal,* 89**:**1 (2008). https://doi.org/10.1016/j.seppur.2007.07.008.

[25] Lesmana S.O., Febriana N., Soetaredjo F.E., Sunarso J., Ismadji S., Studies on Potential Applications of Biomass for the Separation of Heavy Metals from Water and Wastewater, *Biochemical Engineering Journal,* **44**: 19–41 (2009). https://doi.org/10.1016/j.bej.2008.12.009.

[26] Verma R., Dwivedi P., Heavy Metal Water Pollution-A Case Study, *Recent Research in Science and Technology,* **5(5)**: 98-99 (2013).

[27] Vries D., Bertelkamp C., Kegel F.S., Hofs B., Dusseldorp J., Bruins J.H., de Vet W., van den Akker B., Iron and Manganese Removal: Recent Advances in Modelling Treatment Efficiency by Rapid Sand Filtration, *Water Research,* **109**: 35-45 (2017). https://doi.org/10.1016/j.watres.2016.11.032.

[28] Rudi N.N., Muhamad M.S., Chuan L.T., Alipal J., Omar S., Hamidon N., Abdul Hamid N.H., Sunar N.M., Ali R., Harun H., Evolution of Adsorption Process for Manganese Removal in Water Via Agricultural Waste Adsorbents, *Heliyon,* **6(9)**: e05049 (2020). https://doi.org/10.1016/j.heliyon.2020.e05049.

[29] Aziz H.A., Tajarudin H.A., Wei1 T.H.L., Alazaiza M.Y.D., Iron and Manganese Removal from Groundwater Using Limestone Flter with Iron Oxidized Bacteria, *International Journal of Environmental Science and Technology,* (2020). https://doi.org/10.1007/s13762-020-02681-5.

[30] Nguyen V.K., Ha M.-G., Kang H.Y., Nguyen D.D., Biological Manganese Removal by Novel Halotolerant Bacteria Isolated from River Water, *Biomolecules,* **10**: 941 (2020). https://doi.org/10.3390/biom10060941

[31] Fu F., Wang Q., Removal of Heavy Metal Ions from Wastewaters: A Review, *Journal of Environmental Management,* **92(3)**: 407-418 (2011). https://doi.org/10.1016/j.jenvman.2010.11.011.

[32] Meena A.K., Mishra G.K., Rai P.K., Rajagopal C., Nagar P.N., Removal of Heavy Metal Ions from Aqueous Solutions Using Carbon Aerogel as an Adsorbent, *Journal of Hazardous Materials,* **122**: 161-170 (2005). https://doi.org/10.1016/j.jhazmat.2005.03.024.

[33] Ghaedi M., Asadpour E., Vafaie A., Sensitized Spectrophotometric Determination of Cr (III) Ion for Speciation of Chromium Ion in Surfactant Media Using Alpha-Benzoin Oxime, *Spectrochimica Acta*, **63**: 182-88 (2006). https://doi.org/10.1016/j.saa.2005.04.049.

[34] Ali I., Gupta V.K., Advances in Water Treatment by Adsorption Technology, *Nat. Protoc*., **1**: 2661–2667 (2006). https://doi.org/10.1038/nprot.2006.370.

[35] Pyrzynska K., Removal of Cadmium from Wastewaters with Low-Cost Adsorbents, *Journal of Environmental Chemical Engineering*, **7**: 1 (2019). *doi:*10.1016/j.jece.2018.11.040.

[36] Zhu J., Li Y., Xu L., Liu Z., Removal of toluene from Waste Gas by Adsorption-Desorption Process Using Corncob-Based Activated Carbons as Adsorbents, *Ecotoxicology and Environmental Safety,* **165**: 115-125 (2018). *doi:*10.1016/j.ecoenv.2018.08.105.

[37] Pavlík Z., Fořt F., Záleská M., Pavlíková M., Trník, A., Medved I., Keppert M., Koutsoukos P.G., Černý R., Energy-Efficient Thermal Treatment of Sewage Sludge for its Application in Blended Cements, *Journal of Cleaner Production,* **12(1)**:409-41 (2016). https://doi.org/10.1016/j.jclepro.2015.09.072.

[38] Hao X., Chen Q., van Loosdrecht M.C.M., Li J., Jiang H., Sustainable Disposal of Excess Sludge: Incineration without Anaerobic Digestion, *Water Research*, **170**: 115298 (2020). https://doi.org/10.1016/j.watres.2019.115298.

[38] Werther J., Ogada T., Sewage Sludge Combustion, *Progress in Energy and Combustion Science*, **25(1)**: 55-116 (1999). https://doi.org/10.1016/S0360-1285(98)00020-3.

[39] Lin K-L., Chiang K-Y., Lin D-F., Effect of Heating Temperature on the Sintering Characteristics of Sewage Sludge Ash, *Journal of Hazardous Materials,* **128(2-3)**: 175-181 (2006). https://doi.org/10.1016/j.jhazmat.2005.07.051.

[40] Świerczek L., Cieślik B.M., Konieczka P., The potential of Raw Sewage Sludge in Construction Industry – A Review, *Journal of Cleaner Production,* **200**:342-356 (2018). https://doi.org/10.1016/j.jclepro.2018.07.188.

[41] Ooi T.Y., Yong E.L., Md Din M.F., Rezania S., Aminudin E., Chelliapan S., Abdul Rahman A., Park J., Optimization of Aluminium Recovery from Water Treatment Sludge Using Response Surface Methodology, *Journal of Environmental Management,* **228**:13-19 (2018). https://doi.org/10.1016/j.jenvman.2018.09.008.

[42] Ahmad T., Ahmad K., Ahad A., Alam M., Characterization of Water Treatment Sludge and its Reuse as Coagulant, *Journal of Environmental Management,* **182**: 606-611 (2016). https://doi.org/10.1016/j.jenvman.2016.08.010.

[43] Pan S-C., Lin C-C., Tseng D-H., Reusing Sewage Sludge Ash as Adsorbent for Copper Removal from Wastewater, *Resources, Conservation and Recycling,* **39(1)**: 79-90 (2003). https://doi.org/10.1016/S0921-3449(02)00122-2.

[44] Li H., Wang F., Li J., Deng S., Zhang S., Adsorption of Three Pesticides on Polyethylene Microplastics in Aqueous Solutions: Kinetics, Isotherms, Thermodynamics, and Molecular Dynamics Simulation, *Chemosphere,* **264(2)**: 128556 (2021). https://doi.org/10.1016/j.chemosphere.2020.128556.

[45] Yi Z., Liu J., Zeng R., Liu X., Long J., Huang B., Removal of Uranium(VI) From Aqueous Solution by Camellia Oleifera Shell-Based Activated Carbon: Adsorption Equilibrium, Kinetics, and Thermodynamics, *Water Science Technology*; **82(11)**: 2592–2602 (2020). https://doi.org/10.2166/wst.2020.504

[46] Agarwal S., Tyagi I., Gupta V.K., Ghasemi N., Shahivand M., Ghasemi M., Kinetics, Equilibrium Studies and Thermodynamics of Methylene Blue Adsorption on Ephedra Strobilacea Saw Dust and Modified Using Phosphoric Acid and Zinc Chloride, *Journal of Molecular Liquids,* **208**: 208-218 (2016). https://doi.org/10.1016/j.molliq.2016.02.073.

[47] Ho Y.S., Citation review of Lagergren kinetic rate Equation on Adsorption Reactions, *Scientometrics,* **59(1)**: 171-177 (2004).

[48] Freundlich H.M.F., Ueber Die Adsorption in Loesungen, *Zeitschrift fr Physikalische Chemie,* **57**: 385-470 (1907). https://doi.org/10.1515/zpch-1907-5723.

[49] Rajahmundry G.K., Garlapati C., Kumar P.S., Alwi R.S., Vo D-V.N., Statistical Analysis of Adsorption Isotherm Models and its Appropriate Selection, *Chemosphere,* **276:**130176 (2021). https://doi.org/10.1016/j.chemosphere.2021.130176.

[50] Langmuir I., The Adsorption of Gases on Plane Surfaces of Glass, Mica And Platinum, *J. Am. Chem. Soc.,* **40**:1361-1403 (1918).

[51] Budhiary K.N.S., Sumantri I., "Langmuir and Freundlich Isotherm Adsorption Using Activated Charcoal from Banana Peel to Reduce Total Suspended Solid (TSS) Levels in Tofu Industry Liquid Waste", *International Conference on Chemical and Material Engineering (ICCME 2020)", Semarang, Indonesia,* 1053, 012113 (2020).

[52] Brunauer S., Emmett P.H., Teller E., Adsorption of Gases in Multimolecular Layers, *Journal of the American Chemical Society,* **60(2)**: 309–319 (1938). https://doi.org/10.1021/ja01269a023.

[53] Nguyen V.A., Ramanathan M., Application of Brunauer–Emmett–Teller (BET) Theory and the Guggenheim–Anderson–de Boer (GAB) Equation for Concentration-dependent, Non-saturable Cell–Cell Interaction dose-Responses, *J. Pharmacokinet Pharmacodyn*, **47**: 561–572 (2020). https://doi.org/10.1007/s10928-020-09708-x

[54] Temkin M., Pyzhev V., Kinetics of Ammonia Synthesis on Promoted Iron Catalysts, *Acta Physicochimica URSS*, **12**: 327-356 (1940).

[55] Chu, K.H., Revisiting the Temkin Isotherm: Dimensional Inconsistency and Approximate Forms, *Industrial & Engineering Chemistry Research*, **60(35)**: 13140-13147 (2021). https://doi.org/10.1021/acs.iecr.1c01788.

[56] Jones M.E., Nico P.S., Ying S-R., Tom-Thieme J., Keiluweit M., Manganese-Driven Carbon Oxidation at Oxic–Anoxic Interfaces, *Environmental Science & Technology,* **52**:12349-12357 (2018). https://doi.org/10.1021/acs.est.8b03791.

[57] Dada A.O, Olalekan A.P., Olatunya A.M., Dada O., Langmuir, Freundlich, Temkin and Dubinin–Radushkevich Isotherms Studies of Equilibrium Sorption of Zn^{2+} Unto Phosphoric Acid Modified Rice Husk, *Journal of Applied Chemistry,* **3(1)**:38-45 (2012).

[58] Lima E.C., Hosseini-Bandegharaei A., Moreno-Pirajan J.C., Anastopoulos I., A critical review of the Estimation of the Thermodynamic Parameters on Adsorption Equilibria. Wrong Use of Equilibrium Constant in the Van't Hoof Equation for Calculation of Thermodynamic Parameters of Adsorption, *Journal of Molecular Liquids,* **273**: 425-434 (2019). https://doi.org/10.1016/j.molliq.2018.10.048.

[59] Wu C., Adsorption of Reactive Dye onto Carbon Nanotubes: Equilibrium, Kinetics and Thermodynamics, *Journal of Hazardous Materials,* **144**: 93-100 (2007). https://doi.org/10.1016/j.jhazmat.2006.09.083.

[60] Jain S.N., Gogate P.R., Adsorptive Removal of Acid Violet 17 Dye From Wastewater Using Biosorbent Obtained From Naoh and H_2SO_4 Activation of Fallen Leaves of Ficus racemosa, *Journal of Molecular Liquids,* **243**: 132-143 (2017). https://doi.org/10.1016/j.molliq.2017.08.009.

[61] Nie J., Wang Q., Gao S., Poon C.S., Zhou Y., Li J-S., Novel recycling of Incinerated Sewage Sludge Ash (ISSA) and Waste Bentonite as Ceramsite for Pb-Containing Wastewater Treatment: Performance and Mechanism, *Journal of Environmental Management*, **288**: 112382 (2021). https://doi.org/10.1016/j.jenvman.2021.112382.

[62] Elouear Z., Bouzid J., Boujelben N., Removal of Nickel and Cadmium from Aqueous Solutions by Sewage Sludge Ash: Study in Single and Binary Systems, *Environmental Technology*, **30(6)**: 561-570 (2009). https://doi.org/10.1080/09593330902824940.

[63] Schutte N.S., Stilinović E.J., Facilitating Empathy Through Virtual Reality, *Motivation and Emotion,* **41**: 708–712 (2017). https://doi.org/10.1007/s11031-017-9641-7

[64] Shulman B., Dueck R., Ryan D., Breau G., Sadowski I., Misri S., Feasibility of a Mindfulness-Based Cognitive Therapy Group Intervention as an Adjunctive Treatment for Postpartum Depression and Anxiety, *Journal of Affective Disorders,* **235**: 61-67 (2018). https://doi.org/10.1016/j.jad.2017.12.065.

[65] Cohen J., A Power Primer, *Psychological Bulletin,* **12(1)**: 155-159 (1992).

[66] Militaru B.A., Pode R., Lupa L., Schmidt W., Tekle-Röttering A., Kazamer N., Using Sewage Sludge Ash as an Efficient Adsorbent for Pb (II) and Cu (II) in Single and Binary Systems, *Molecules,* (2020). https://doi.org/10.3390/molecules25112559.

[67] Coutand M., Cyr M., Clastres P., Use of Sewage Sludge Ash as Mineral Admixture in Mortars, *Proceedings of the Institution of Civil Engineers Construction Materials,* **159**: 153–162 (2006). https://doi.org/10.1680/coma.2006.159.4.153.

[68] Mahieux P.Y., Aubert J.E., Cyr M., Coutand M., Husson B., Quantitative Mineralogical Composition of Complex Mineral Wastes-Contribution of the Rietveld Method, *Waste Management,* **30**: 378–388 (2010). https://doi.org/10.1016/j.wasman.2009.10.023.

[69] Chen Z., Li J-S., Zhan B-J., Sharma U., Poon C.S., Compressive Strength and Microstructural Properties of Dry-Mixed Geopolymer Pastes Synthesized from GGBS and Sewage Sludge Ash, *Construction and Building Materials*, **182**: 597-607 (2018). https://doi.org/10.1016/j.conbuildmat.2018.06.159